

Dual Solution Synthesis of Alloyed Compound Thin Films of $\text{CuCdPbS}_2\text{O}_4$ for Possible Device Applications

Joseph Ijeoma Onwumeka, Ph.D.^{1*}, Okechukwu Kelechi Nwofor, Ph.D.², and Ngozi Patricia Ebosie, M.Sc.³

¹Department of Physics, Imo State University, Owerri, Nigeria. Postal code 460222.

²Department of Physics, Imo State University, Owerri, Nigeria. Postal code 460222.

³Department of Chemistry, Imo State University, Owerri, Nigeria. Postal code 460222.

*Corresponding Author

Received: 23 November 2021; Accepted: 22 February 2022; Published: 08 April 2023

Abstract: - The need to improve on the basic applications on already existing binary and ternary thin films led to the development of compound material of $\text{CuCdPbS}_2\text{O}_4$ alloyed thin films through the simultaneous combinations of CuS, CdO and PbS thin films derived from their different precursor materials. $\text{CuCdPbS}_2\text{O}_4$ alloyed thin films have been fabricated on 76mm x 26mm x 1mm commercial-quality glass microscopic substrates using dual solution synthesis (DSS) from aqueous solutions of precursor materials of hydrogen peroxide (H_2O_2), hydrated copper sulphate (CuSO_4), cadmium chloride (CdCl_2), lead nitrate ($\text{Pb}(\text{NO}_3)_2$) and thiourea in which aqueous ammonia solution was employed as complexing agent. The samples were annealed at the temperatures, of 100 °C, 150 °C, 200 °C, and 250 °C.

The crystallographic studies were done using X-ray diffractometer (XRD) and scanning electron microscope (SEM). The XRD patterns of $\text{CuCdPbS}_2\text{O}_4$ alloyed thin films of samples A and B have diffraction peaks at $2\theta=12.89^\circ$ and $2\theta=24.93^\circ$. The grain sizes of samples A and B are 89.690nm and 62.733nm respectively. The deposited film compound with chemical formula $\text{CuCdPbS}_2\text{O}_4$ has dickite structure with monoclinic crystal system. Sample A, B, C and D have low optical transmittance in the ultraviolet region, high in the visible and high in the near infrared regions of electromagnetic spectrum.

The two samples, have average direct wide band gap of $3.91\pm 0.05\text{eV}$. The films can be found useful in cold and heat mirror applications, active layer in various types of solar cells, liquid crystal displays, flat panel displays for optoelectronic applications, gas sensor, photovoltaics, photoconductive cells and photo-electrochemical sensing devices.

Keywords: Transmittance, Band Gap, Absorbance, Reflectance, Optical Conductivity, Photovoltaic

I. Introduction

Thin films play important roles in contemporary electronics and optoelectronic applications. In the early days of radio and television transmitting and receiving equipment relied on vacuum tubes, but these have almost been completely replaced in the last four decades by semiconducting materials, including transistors, diodes, integrated circuit and other solid state devices.

Transition metal chalcogenides such as cadmium and copper are important inorganic materials with wide range of potential applications in the magnetic, electronics, catalytic and optical industry [1]. These materials can be divided into two categories: layered materials with Van der wall's spacing between the layers, which comprise two-third of transition metal chalcogenides and non-layered materials [2]. The transition metal chalcogenides (TMC) is a family of compounds with the formula M_yX_z , where M is a member of transition metals (V, Nb, Ta, Cr, Mo, W, Mn, Tc, or Re), while X represent a member of chalcogen family (P, S, Se and Te), y and z are integers. They have a variety of potentially useful properties [3,4].

Depending on the transition metal and the chalcogen involved, layered transition metal chalcogenide (LTMC) can have properties ranging from semiconducting to superconducting layered bulk chalcogenide crystal materials and are composed of vertically stacked layers bonded together by weak van der Waals forces, similar to the van der Waals forces in graphite [5]. Owing to strong surface effects, the properties of the materials vary drastically with the number of layers in a sheet. The electrical and optical properties of these compounds can be tuned on demand by reducing or increasing the number of layers [6], which makes them potential candidates for tunable nano-electronics [7].

Copper sulphide is a promising material for optoelectronics and photovoltaics. During the growth of ultrafine functional layers of Cu_xS , the electronic structure of sulphide is determined primarily by the crystallographic orientation of a substrate and by the method being applied. It can be classified into three groups, namely monosulphide, disulphide and mixed monosulphide. Copper sulphide occurs naturally in nature as a mineral called covellite. It conducts electricity moderately [8]. Both synthetic materials and

minerals contain copper sulphide. It has a band gap of 1.21eV and hole mobility of 5.5-9cm²/V. CuS as a semiconducting material has a nonlinear optical properties [9], with increasing conductivity at high temperature, excellent solar radiation absorbing properties and high capacity cathode material in lithium secondary batteries [10]. Based on the fact that copper sulphide is a material for optoelectronics and photovoltaics, it finds applications in the following photoelectrical devices and electronics: solar cells, superionic conductors, photo detectors, electro-conductive electrodes, photo-thermal conversion devices, microwave shielding coating, active absorbents of radio waves, gas sensors, polarizer of infrared radiation, etc.

CdO thin film is an n-type semiconductor with rock-salt crystal structure (FCC) and has a direct band gap of 2.2eV. CdO belongs to group II-VI semiconductor materials with immense applications in optoelectronics [11]. CdO nanoparticles are known to be highly reactive and they have been employed in processes such as energy storage system, electro chromic thin films, magnetoresistive devices and heterogeneous catalysis. In nanoscience and nanotechnology synthesis forms an essential component infrared filter for heat and cold windows. Nanomaterials which have been generated by chemical methods have proven to be more effective, providing better control as well as enable different sizes, shapes and functionalization than those generated with such physical methods as laser ablation, arc-discharge and evaporation. Metal oxide nanoparticles can be produced by soft chemical methods, such as co-precipitation, sol-gel and hydrothermal synthesis. Cadmium is a shiny metal with a bluish cast (shade) to it. Its melting point is 321°C (610 °F) and its boiling point is 765 °C (1,410 °F). The density of cadmium is 8.65 grams per cubic centimeter. The sensing properties of nanostructured CdO thin films have been studied for liquefied petroleum gas (LPG) at operating temperature of 573 K. The CdO thin films exhibited maximum gas response of 44% upon the LPG exposure of 1040 ppm [12].

Lead sulphide (PbS) is an important direct narrow gap semiconductor material with a band gap of 0.4 eV and has a cubic structure. Due to their suitable band gaps, PbS thin films are extensively used in IR detectors. Lead sulphide (PbS) is an important IV-VI group chalcogenides that has attracted considerable attention in the recent times due to its numerous optical and opto-electronic properties and useful applications in solar cells, optoelectronic devices, photoconductors, sensors and infrared detector devices. PbS thin films has direct optical band gap that can be changed from 0.39 up to 5.20eV. PbS thin films have been deposited through various deposition processes such as spray pyrolysis [13,14], chemical bath deposition [15], and successive ionic layer adsorption and reaction [16].

The major objectives in preparing this material compound thin films are to study the optical, structural, annealing, elemental compositions and thickness measurements of the alloyed thin films of CuCdPbS₂O₄ and the possible applications in both electrochemical sensing, photo sensing, photovoltaics, photoconductivity and other passive applications such as cold and heat window coatings, coatings on eye glasses, tint on vehicle windscreen, heater, gas sensor and detectors.

Table 1 Parameters and samples produced by SILAR and solution growth technique

Samp les	Dep. Time (h)	NH ₃ Conc. (mol)	CuSO ₄ Conc. (mol)	CdCl ₂ Conc. (mol)	Pb(NO ₃) ₂ Conc. (mol)	H ₂ O ₂ Conc. (mol)	NH ₃ soln Conc. (ml)	CuS O ₄ Vol. (ml)	CdCl ₂ Vol. (ml)	Pb(NO ₃) Vol. (ml)	Thiourea Vol. (ml)	H ₂ O ₂ Vol. (ml)	Annealing Temp. (°C)	Dep. Temp. (°C)
A	3.0	3.0	0.2	0.1	0.2	1.0	4.0	20.0	20.0	20.0	11.0	9.0	100	20
B	3.0	3.0	0.2	0.1	0.2	1.0	4.0	20.0	20.0	20.0	11.0	9.0	150	20
C	3.0	3.0	0.2	0.1	0.2	1.0	4.0	20.0	20.0	20.0	11.0	9.0	200	20
D	3.0	3.0	0.2	0.1	0.2	1.0	4.0	20.0	20.0	20.0	11.0	9.0	250	20

II. Materials and Method

Table 1 shows the parameters employed for dual solution synthesis in the deposition of CuCdPbS₂O₄ which involves the deposition of CuS and CdO thin films using SILAR method followed by immersing the substrates containing the deposits of CuS and CdO into the solution containing suspected PbS and were allowed to remain for 3 h. For the deposition of CuCdPbS₂O₄ thin films, 20 ml of aqueous solution of lead nitrate, 20 ml of aqueous solution of copper sulphate and 20 ml of aqueous solution of cadmium chloride were used as cationic precursor and 9 ml of hydrogen peroxide and 11 ml of aqueous solution of thiourea as the anionic precursors.

4 ml of aqueous solution of NH₃ (ammonium hydroxide) as complexing agent was measured and was added to the precursor solutions.

To grow CuCdPbS₂O₄ thin films, the substrates were immersed in CuSO₄:5H₂O solution with aqueous solution of NH₃ as complexing agent for 5s where Cu²⁺ were adsorbed on the surface of the microscopic glass substrates. In the second stage, the substrates were rinsed for 5 s in de-ionized water to remove loose and unadsorbed Cu²⁺ ions from the surfaces of the substrates. The substrates were then removed and immersed in thiourea solution for 5 s, where the S²⁻ ions reacted with adsorbed Cu²⁺ ions on the substrates surfaces to form CuS layer. This is given in equations (1) and (2).

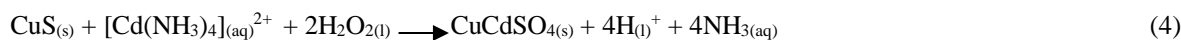
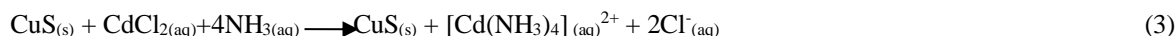
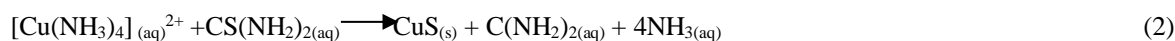
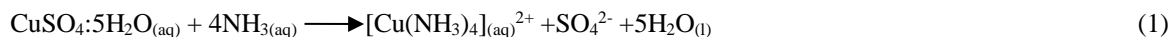
Finally, the substrates were again rinsed in die-ionized water to remove loose and un-adsorbed atoms from the substrates' surfaces. Afterwards the substrates were immersed in Cadmium chloride solution with NH₃ as a complexing agent for 5 s to adsorb Cd²⁺ ions on the already adsorbed CuS layer as give in equations (3)and (4).

The un-adsorbed cadmium ions were removed from the substrates by rinsing in de-ionized water for 5s.The substrate was then immersed in hydrogen peroxide solution for 5 s where O²⁻ ions reacted with cadmium to form a layer of CdO. The substrates were immersed in already prepared solution of lead tetra-amine complex ion in the presence of thiourea solution for 1hr for the deposition of PbS on the substrate containing CuS and CdO, which lead to the formation of CuCdPbS₂O₄ compound thin films and is given in equation (5). Equation (5) signifies the involvement of the second method known as solution growth technique, which combines with SILAR method to bring about what is known as Dual Solution Synthesis (DSS).

2.1. Reaction Mechanism

The reaction stages leading to the formation of CuCdPbS₂O₄ are of two stages and are given as follows:

2.1a SILAR Process



2.1b Solution Growth Technique (SGT) Process



III. Results and Discussion

The depositions on microscopic glass substrates have been successfully achieved, the deposited samples were annealed to remove water of crystallization. The annealing of the samples were done at varying temperatures of 100 °C, 150 °C, 200 °C and 250 °C for 1 hour. The thicknesses of the samples, A, B, C and D as grown under the room temperature of 20 °C, were measured by optical method are 132.49 nm, 122.67 nm, 115.54 nm and 105.34 nm respectively. As it can be observed, the thicknesses of the samples decrease as the annealing temperatures increase.

3.1. Crystallographic Study of Samples A and B

Samples A and B are selected as representative samples for the studies of structures and morphologies of the deposited samples. X-ray diffraction of samples A and B are measured using Miniflex 600 by Rigaku Cooperation Japan. XRD patterns of CuCdPbS₂O₄ of samples A and B grown under the same conditions have one diffraction peak each at 2θ = 12.89 ° and 2θ = 24.93 ° respectively. The grain sizes of samples A and B of the alloy are 89.690 nm and 62.733 nm respectively. A new compound thin film of CuCdPbS₂O₄ with dickite structure and of monoclinic crystal system. This material has close resemblance to Niedermayrite (Giester *et al.*, 1998), but not exactly. These are shown in Figures 1 and 2. This implies that the deposited material is a new alloyed substance.

3.2. Morphological and Elemental Compositions of Samples A and B

The morphological studies of samples A and B were determined using Phenom Proxy by Phenom World Eindhoven, Nethertland. Sample A as revealed by scanning electron microscope (SEM) in Figure 3 shows that it has smooth dark surface with white spots which indicate the inter-atomic interactions between the constituent atoms that made up the emergent thin film compound which shows the bonding strength of the material. The EDX as shown in Table 1 gives the various atomic concentrations of the deposited material. The add-atoms are: Cu=0.52 mol/dm³, Cd=0.57 mol/dm³, Pb=1.02 mol/dm³, S=0.74 mol/dm³ and O=6.03 mol/dm³. The other atomic concentrations in Table 2 are associated with the substrates and the trace elements found in the reagents.

Figure 4 is the image of sample B as studied by scanning electron microscope, it shows that the deposited sample has a smooth surface with near uniform surface having tiny white spots. The material exhibits interactions of combining substances during chemical reactions. EDX as depicts in Table 3, the concentrations of the add-atoms are: Cu= 0.23 mol/dm³, Cd=0.32 mol/dm³, Pb=0.89 mol/dm³, S=0.58 mol/dm³ and O=8.39 mol/dm³. The other atomic concentrations in Table 2 are associated with the substrates and the trace elements found in the reagents

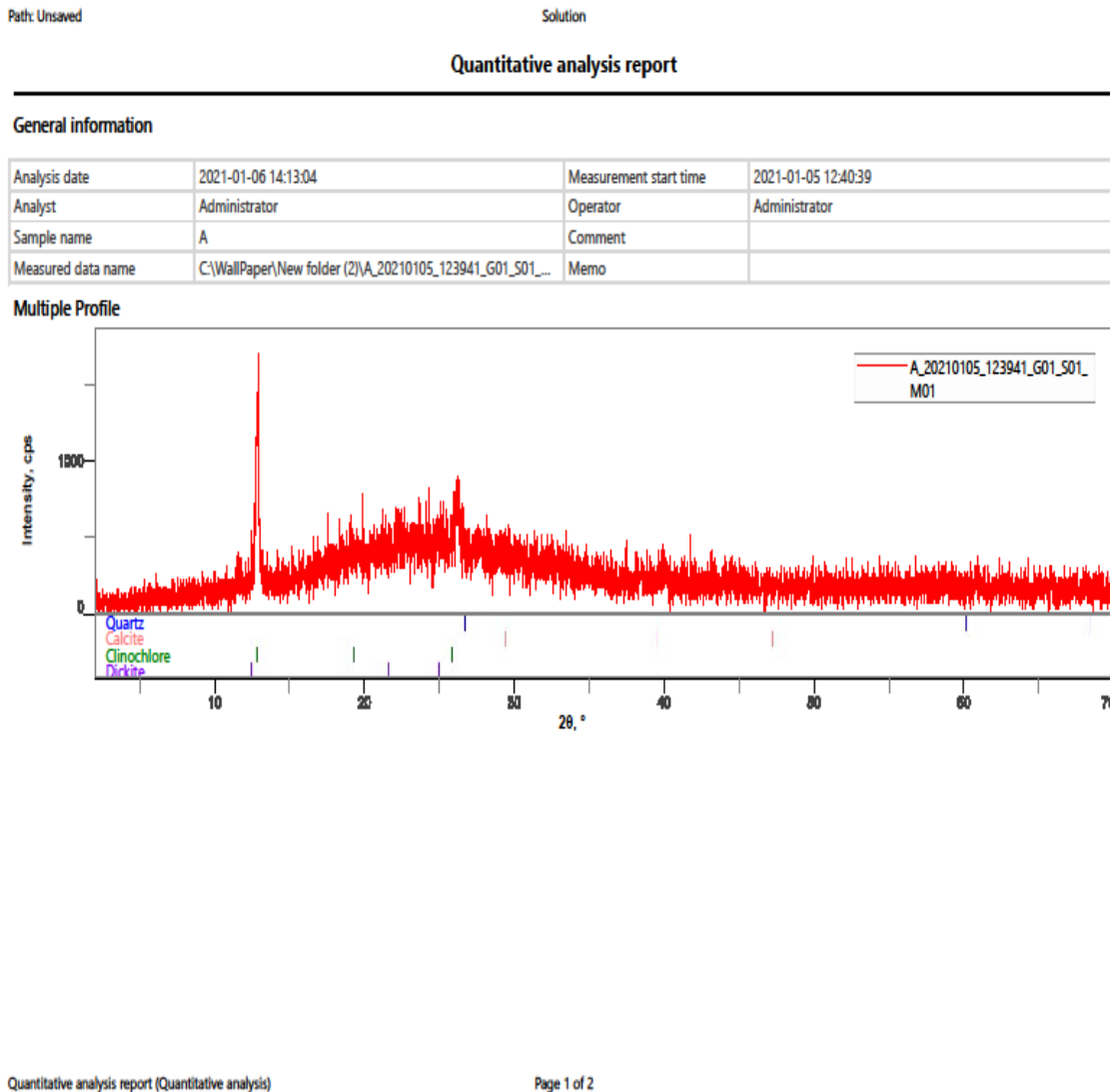


Figure 1 X-ray Diffraction of sample A

Path: Unsaved

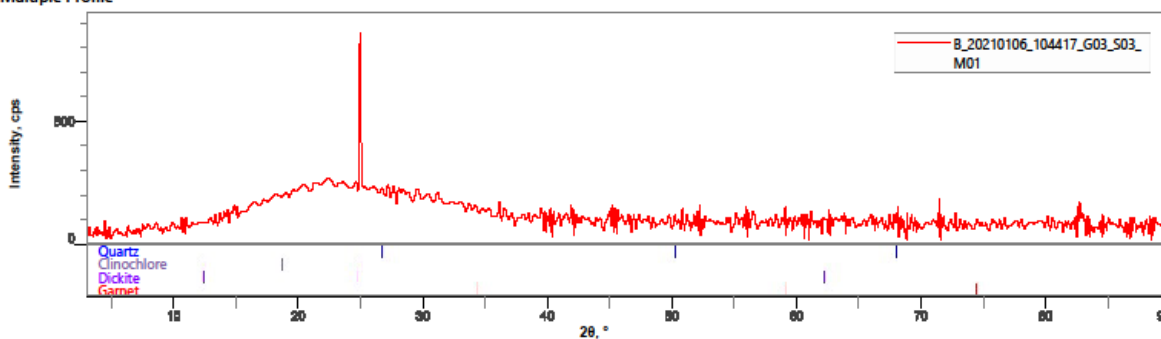
Solution

Quantitative analysis report

General information

Analysis date	2021-01-06 14:36:12	Measurement start time	2021-01-06 10:45:28
Analyst	Administrator	Operator	Administrator
Sample name	B	Comment	
Measured data name	C:\WallPaper\New folder (2)\B_20210106_104417_G03_S03_...	Memo	

Multiple Profile



Quantitative analysis report (Quantitative analysis)

Page 1 of 2

Figure 2 X-ray Diffraction of sample B

Table 2 Atomic Concentrations of sample A

Element Number	Element Symbol	Element Name	Atomic Conc.	Weight Conc.
14	Si	Silicon	58.84	52.80
20	Ca	Calcium	10.44	13.36
11	Na	Sodium	10.43	7.66
82	Pb	Lead	1.02	6.78
12	Mg	Magnesium	4.22	3.28
8	O	Oxygen	6.03	3.08
47	Ag	Silver	0.71	2.45
19	K	Potassium	1.75	2.18
48	Cd	Cadmium	0.57	2.03
13	Al	Aluminium	2.35	2.02
17	Cl	Chlorine	1.29	1.46
15	P	Phosphorus	1.09	1.08
29	Cu	Copper	0.52	1.05
16	S	Sulfur	0.74	0.76
22	Ti	Titanium	0.00	0.00
26	Fe	Iron	0.00	0.00
30	Zn	Zinc	0.00	0.00

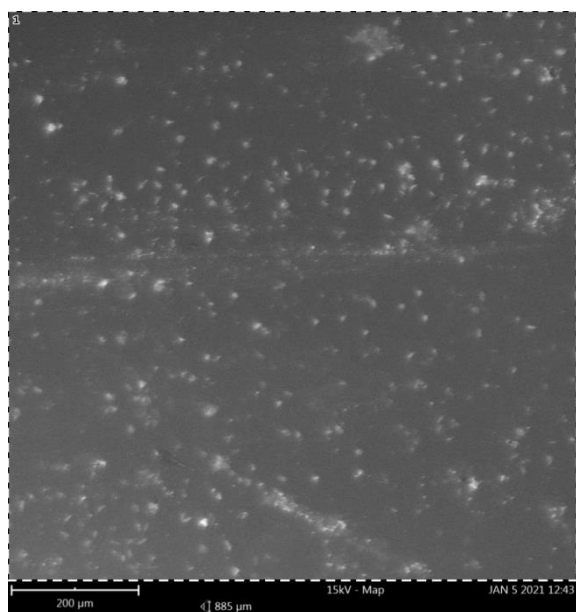


Figure 3 SEM of sample A

Table 3 Atomic Concentrations of Sample

Element Number	Element Symbol	Element Name	Atomic Conc.	Weight Conc.
14	Si	Silicon	59.45	55.08
20	Ca	Calcium	10.15	13.43
11	Na	Sodium	10.24	7.77
82	Pb	Lead	0.89	6.11
8	O	Oxygen	8.39	4.43
12	Mg	Magnesium	4.02	3.22
47	Ag	Silver	0.63	2.24
13	Al	Aluminium	2.23	1.98
19	K	Potassium	1.26	1.62
48	Cd	Cadmium	0.32	1.17
17	Cl	Chlorine	0.88	1.03
16	S	Sulfur	0.58	0.61
15	P	Phosphorus	0.59	0.60
29	Cu	Copper	0.23	0.48
22	Ti	Titanium	0.14	0.22
26	Fe	Iron	0.00	0.00
30	Zn	Zinc	0.00	0.00

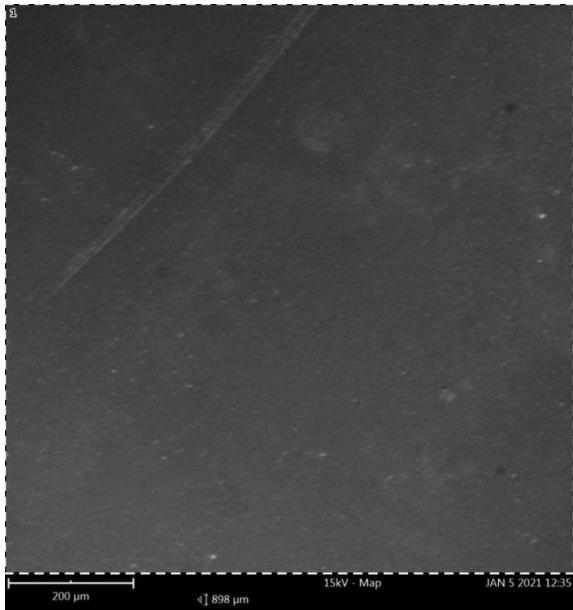


Figure 4 SEM of Sample B

3.3. Optical Measurements

The optical characterization of the four samples were measured using UVI double beam spectrophotometer with serial number 1800, the transmittance which is the ratio of the incident intensity to the transmitted intensity of the radiation was taken as the default. The samples were scanned for transmittance from UV (ultraviolet), through visible to near infrared regions of electromagnetic spectrum. The absorbance, reflectance, and energy band gap were adequately determined from relevant equations.

3.3a Transmittance (T)

The transmittance increases from 0.13 to 0.79 as the wavelength increased from 299nm to 900nm. Samples A,B, C, D share similar characteristics as indicated in Figure 5. The transmittance increases from the lowest values at the UV, and increases through the visible to near infrared region of electromagnetic spectrum, and can be used as heat and cold window in infrared optics, photo-conducting materials, due to its high transmittance, as UV shielding material in cream and paint production due to its low transmittance at the UV region, tint on glass windows, eyeglasses, car windscreen and as warmer in poultry house.

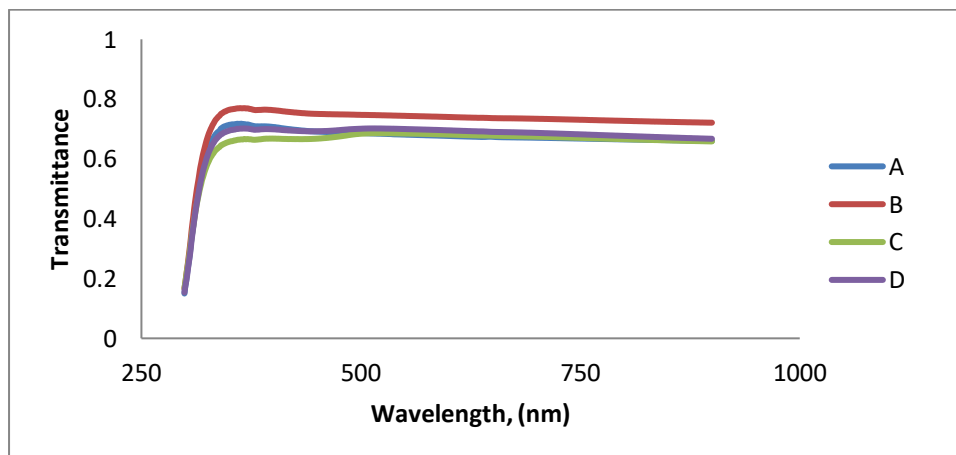


Figure 5 Graph of transmittance against wavelength

3.3b Absorbance

There is fall of absorbance for all the samples with increase in wavelength which indicates a shift from a region of more absorbance to a region of less absorbance as shown in Figure 6. Samples A, B, C, D have similar characteristics as indicated in the graph while sample B has the lowest absorbance, the range is from 0.24 to 0.59. Samples A, B, C, D can be used in production of electrochemical sensing devices for detection of harmful and useful gaseous substances and in the UV spectroscopy for the studies of different atomic, molecular, solar spectra etc.

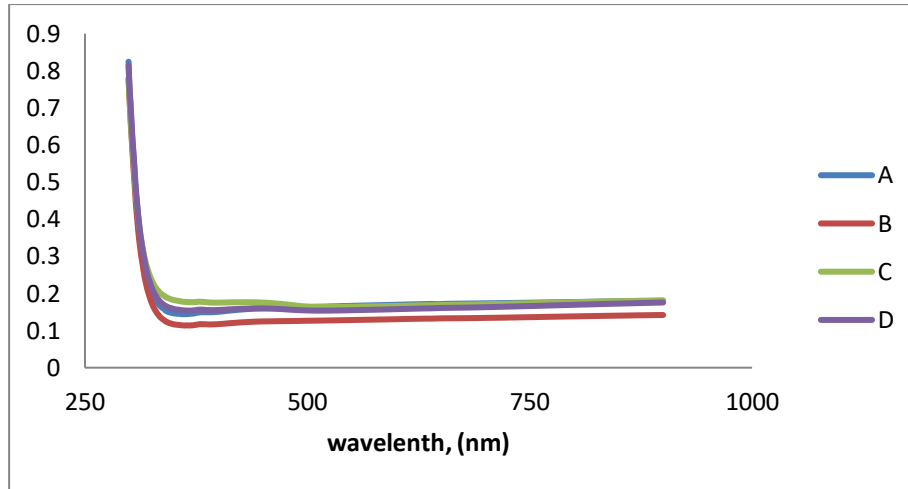


Figure 6 Graph of absorbance against wavelength

3.3c Reflectance

The reflectance of the samples increased from 0.02 to 0.20 and generally the reflectance is relatively low. It can therefore be used in multi-layer thin film technology for antireflection coatings of almost zero reflectance in the visible region, for solar energy collectors. The graph of reflectance R for the samples is shown in the Figure 7.

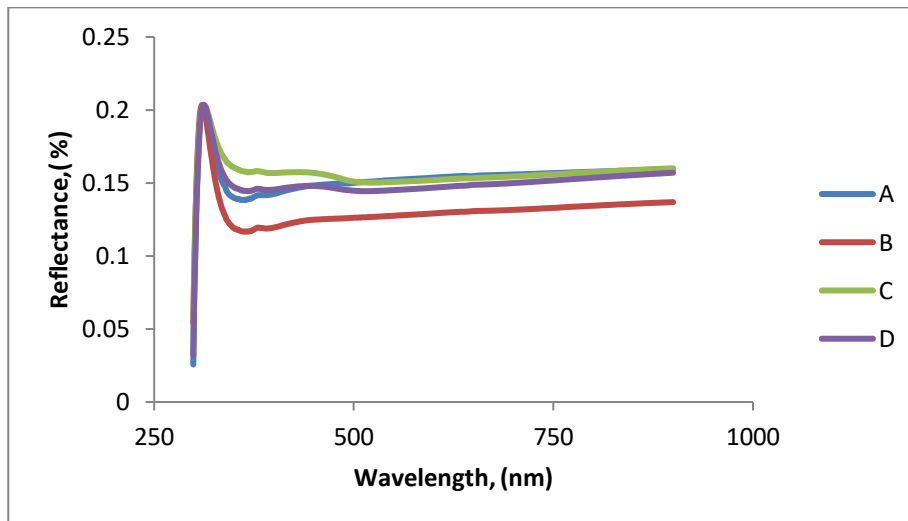


Figure 7 Graph of reflectance against wavelength

3.3d Energy band gap (E_g)

The band gap is determined from the graph of $(\alpha h\nu)^2$ against photon energy $h\nu$, by extrapolating the straight portion of the curve where $\alpha h\nu = 0$ as plotted in Figure 8. The average band gap of the four samples is 3.91 ± 0.05 eV. The high energy band gap of the samples may be due to adequate absorption that exist between the atomic components that made up the deposited compound material. This material with wide energy band gap, can be found applicable in photo-electronics, photovoltaics, thin film electrodes, thin film photoconductors, liquid crystal displays for optoelectronic applications.

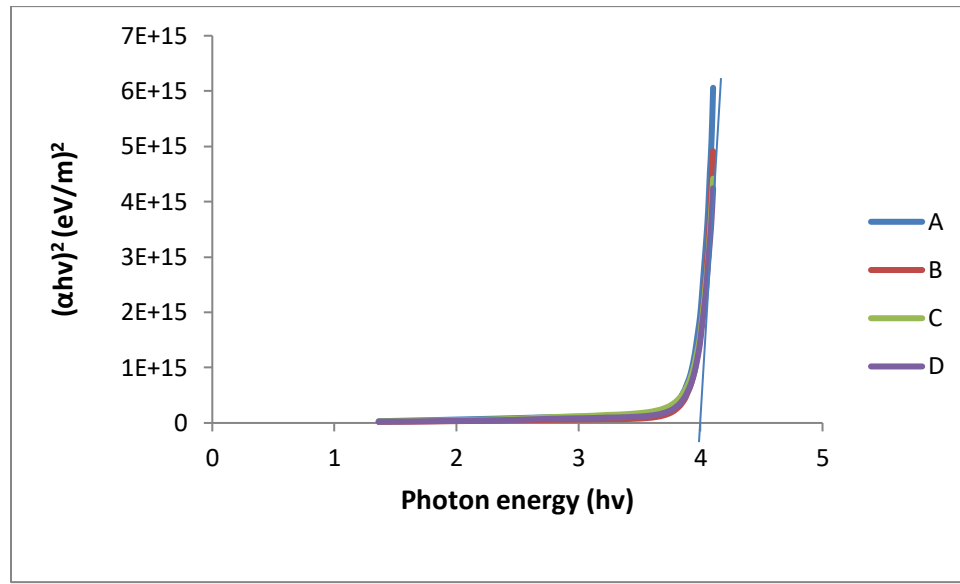


Figure 8 Graph of $(\alpha hv)^2$ against Photon Energy hv

IV. Conclusion

The $\text{CuCdPbS}_2\text{O}_4$ thin films have successfully been deposited on glass substrates. This was achieved using Dual Solution Synthesis (DSS) which was preferred over other solution deposition techniques because of its combination of the dual properties of SILAR and Solution Growth Technique (SGT). It is cheap, effective, accurate and easy to execute.

The substrates were prepared in aqua regia before been used for the deposition. The complexing agent used is ammonia (NH_3) and the precursor materials used as the sources of cations are solutions of $\text{Pb}(\text{NO}_3)_2$, hydrated CuSO_4 , CdCl_2 . Thiourea and H_2O_2 are the major sources of anions.

The deposition of $\text{CuCdPbS}_2\text{O}_4$ was carried out at room temperature of 20°C . The samples were annealed at 100°C , 150°C , 200°C and 250°C for 1hour. The structures of deposited thin films were studied using XRD and SEM.

The graphs of the optical characterization were plotted against wavelength for the four samples produced. The energy band gaps of the samples was determined from the graph of $(\alpha hv)^2$ against hv by extrapolation of straight portion of the curves to hv axis where $(\alpha hv) = 0$. The average band gap of the four samples is $3.91 \pm 0.05\text{eV}$. As a material with wide energy band gap, it can be found useful as photo-electrochemical, photovoltaic and photoconductive thin film material for optoelectronic applications, solar cell production, sensor devices, chemical detectors in oil and gas productions and passively be considered as material for solar control coatings.

Acknowledgements

The funding of this research was made possible through the intervention of TETFUND's Institution Base Research (IBR) grant. Our utmost appreciation goes to the body.

Our profound gratitude, goes to our Institution, Imo State University, Owerri Nigeria for the provision of conducive environment, including thin film laboratory in the Department of Physics where the experimental exercise was carried out.

We are grateful to the laboratory officials of Obafemi Awolowo University Ile-Ife Nigeria in the persons of Prof. I.E. Obiajunwa of Centre for Energy Research and Development and Mr. E.A. Akinola of Central Science Laboratory, of Obafemi Awolowo University, Ile-Ife, Nigeria, for their assistance in successful realization of this work.

The team also wishes to appreciate the contribution of Mr. Isa Yakubu of Chemical Engineering Department, of Ahmadu Bello University Zaria, Nigeria.

Conflict of interests

No competing interest among the authors

Authors' information**Joseph Ijeoma Onwuemeka, PhD**

Department of Physics

Imo State University, Owerri, Nigeria

Interest Areas Include: Condensed Matter Physics-Thin Films,
Nanostructure Materials, Solar Cells, Hybrid Materials,
Medicinal Plants Extracts for Disease Control and Hybrid Medicines

Okechukwu Kelechi Nwofor, PhD

Department of Physics

Imo State University, Owerri, Nigeria

Interest Areas Include; Atmospheric Physics- Aerosols,
Environmental Geophysics and Solar Energy Physics

Ngozi Patricia Ebosie, MSc

Department of Chemistry

Imo State University, Owerri, Nigeria

Inorganic Chemistry and Materials Science

Reference

1. Umair S, Raja A H and Amin B 2016 *J. Sol. Chem.* **238** 25
2. Weck P F, Kim E and Czerwinski K R 2013 *J. Dalton Transact.* **42** 15288
3. Benameur M, Radasavljevic B, Heron J, Sahoo S and Berger H 2011 *J. nanotech.* **22** 125
4. McCandless B and Dobson K 2004 *J. Solar Energy* **77** 839
5. Novoselov K, Geim A, Morozov S, Jiang D, Zhang Y, Dubonos S *et al* 2004 *J. of Thin Film Sci.* **306** 669
6. Han S, Kwon H, Kim S, Ryu S, Yun W, Kim D *et al* 2011 *J. Physic. Rev.* **84** 45
7. Johari P and Shenoy V 2012 *J. ACS Nanotech.* **6** 5449
8. Sabah F A, Ahmed N M and Hassan Z 2017 *J. Electron. Mater.* **46** 218
9. Poulomi R and Suneel K S 2006 *J. Cryst. Growth and Design* **6** 1921
10. Chung J S and Sohn, H J 2002 *J. Power Sources* **108** 226
11. Sahin B, Bayansal F, Yunsel M and Getinkara H A 2014 *Mater. Sci. Semicond. Proc.* **18** 135
12. Bulankhe and Lokhande 2013 *Sensors and Actuators B: Chemica*, **200** 245
13. Thangarajju B and Kaliannan P 2000 *Semicond. Sci. Technol.* **159** 849
14. Abdallah B, Ismail A, Kashoua H and Zetoun W 2018 *J. Nanomater.* **6** 1
15. Sandip V, Bhatt M P, Deshpande B H S, Nitya G and Sunil H C 2013 *Sol. Stat. Phenom.* **209** 111
16. Mosiori C O, Njoroge W N and Okumu J 2014 *Int. J. Adv. Res. in Physic. Sci. (IJARPS)* **1** 25